Available online at www.sciencedirect.com
SCIENCE DIRECT
International Journal of Mass Spectrometry 249–250 (2006) 77–92
International Journal of Mass Spectrometry
www.elsevier.com/locate/ijms

Gram-negative bacterial lipid A analysis by negative electrospray ion trap mass spectrometry: Stepwise dissociations of deprotonated species under low energy CID conditions

Geoffrey Madalinski[a,b], Françoise Fournier[b], Franck-Lionel Wind[a], Carlos Afonso[b], Jean-Claude Tabet[b,*]

[a] *Centre d'Etudes du Bouchet, BP 3, 91710, Vert-le-Petit, France*
[b] *Université Pierre & Marie Curie, 4 place Jussieu, boite 45, 75252 Paris Cedex 05, France*

Received 3 November 2005; received in revised form 21 December 2005; accepted 27 December 2005
Available online 14 February 2006

Abstract

After mild acid hydrolysis of the lipopolysaccharide (LPS) from *Escherichia coli* J5, the recovered underivatized lipid A was analyzed using an electrospray source coupled with an ion trap mass analyzer (ESI-ITMS). Our work deals with the study of these complex endotoxic biomolecules under CID conditions. Sequential MS^n experiments with the ion trap instrument allowed the characterization of the substituting side chain. Mono- and diphosphorylated singly or doubly deprotonated lipid A molecules have been studied and provided complementary information. The experimental results obtained, from these negatively charged species, under low energy collision conditions motivated us to propose stepwise fragmentation pathways involving intermediate ion–dipole complexes. In this way charge-driven processes are considered instead of the charge-remote mechanisms usually proposed in the literature.

Keywords: Lipid A; Electrospray; Ion–dipole; Ion trap mass spectrometry; Low energy collision

Endotoxic lipopolysaccharides (LPS), in addition to phospholipids and proteins [1], are the major components of the outer membrane of all Gram-negative bacteria. These molecules, responsible for the harmful prokaryotic cell activity of these micro-organisms, are highly immunogenic and directly involved in numerous bacterial diseases in humans such as Gram-negative sepsis [2]. Their structural study by mass spectrometry contributes to the understanding of processes related to bacterial pathogenesis, combined to the characterization and identification of these prokaryotic cells. The full structure of endotoxins in their smooth form (S-type) consists of three covalently linked regions [3–6]: a lipid A moiety and two variable glycosidic domains. The lipid A which anchors the LPS at the outer surface is a glucosamine dimer [D-GlcN- β(1′ → 6)-D-GlcN] skeleton. It is (i) N- and O-acylated at the C-2, C-3, C-2′ and C-3′ positions by up to seven C_{10}–C_{18} fatty acid (mainly the 3-hydroxy and acyl-oxy-acyl fatty acids) and (ii) phosphorylated at the C-1 and C-4′ positions of the disaccharide ring. The oligosaccharide core linked to the C-6′ position of the lipid A backbone is made up of several sugar units such as neutral hexoses (glucose, galactose), heptose (L-glycero-D-manno heptose) and 3-deoxy-D-manno-2-octulosonic acids (Kdo). In addition, the O-specific chain is built up with up to seven sugar repeating units and is considered as an outer cell antigenic determinant.

Over the last two decades, the structural characterization of LPS was carried out by NMR [7,8] and by mass spectrometry using various desorption techniques. Firstly, fast atom bombardment (FAB) [9,10], laser desorption (LD) [11–13] and plasma desorption (PD) [14,15] as early soft ionization methods, permitted the first characterization of the lipid A structure. But more recently, very soft desorption/ionization techniques such as matrix-assisted laser desorption/ionization (MALDI) [16,17] and electrospray (ESI) [18–20] enabled the analysis of such biomolecules by reducing the internal energy of desorbed molecular species and thus, hindering gas phase fragmentations and

* Corresponding author. Tel.: +33 1 44 27 32 63; fax: +33 1 44 27 38 43.
E-mail address: tabet@ccr.jussieu.fr (J.-C. Tabet).

1387-3806/$ – see front matter © 2006 Elsevier B.V. All rights reserved.
doi:10.1016/j.ijms.2005.12.049

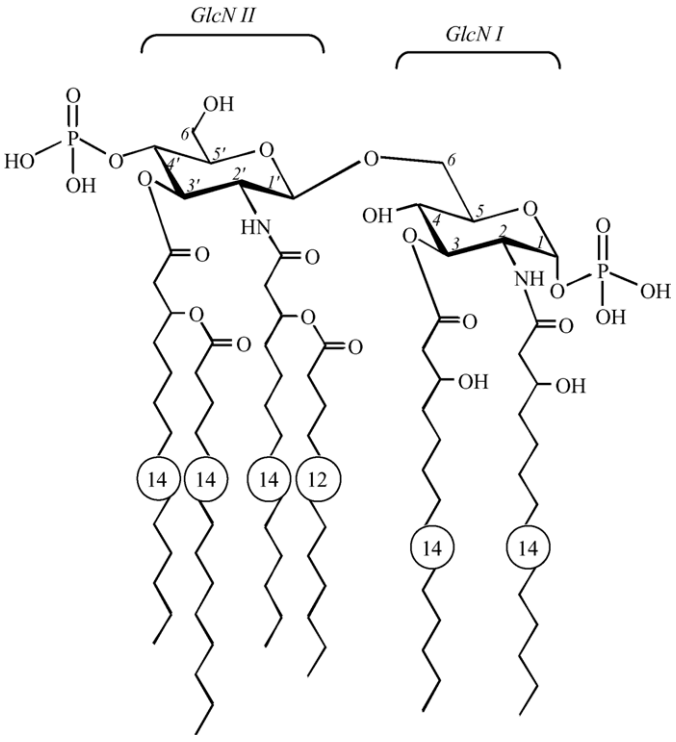

Scheme 1. Structure of the diphosphoryl lipid A (DPLA) from *E. coli*.

allowing the determination of a more accurate molecular structure.

The structure of the *E .coli* type lipid A is composed of a diphosphorylated disaccharide backbone substituted, for the major species, by six fatty acid chains following the degree of acylation of this expressed heterogenic molecule. The hexaacyl component (Scheme 1) bears two chains in amide linkage at the C-2 and C-2′ positions: (i) a (*R*)-3-hydroxymyristic acid [C14:0(3-OH)] substituting the GlcN I ring at the C-2 position and (ii) a (*R*)-3-hydroxymyristic acid O-acylated by either a lauric acid [C14:0(3-O(12:0))] or an hydroxylauric acid [C14:0(3-O(12:0(3-OH)))] substituting the GlcN II ring at the C-2′ position. In addition, the lipid A is substituted by ester linkages: (i) a (*R*)-3-hydroxymyristic acid [14:0(3-OH)] chain at the C-3 position and (ii) a (*R*)-3-hydroxymyristic acid which is O-acylated by a myristic acid [14:0(3-O(14:0)] at the C-3′ position.

The aim of our study, performed with an ESI-ion trap instrument, is the structural analysis of a well-known lipid A widely used as a model, in order to point out the existence of molecular heterogeneities in the fatty acid chains. To document heterogeneities, negative ion ESI mode was mainly used because of the presence of the easily deprotonated phosphate groups in the gas phase. Furthermore, the source and trapping conditions were modified in to optimize the various mass-to-charge ratio ranges.

Lipid A contains one or two phosphoryl group(s), considered to be very acidic in the gas phase [21]. The phosphate substitute(s) the N-acetylglucosamine disaccharide at the C-1 and/or C-4′ position(s). Therefore, under negative ion mode, the production of deprotonated molecules is favored [20]. From the doubly phosphorylated molecules, the ESI processes lead to the formation of doubly deprotonated lipid A [22]. Into the ion trap cell, the application of the resonant excitation voltage on the selected singly and doubly charged precursor ions, yields diagnostic product ions. The fingerprint investigation of the CID spectra of $[M-H]^-$ ions enabled an accurate structural determination especially using sequential MS^n analysis. In order to simplify the study of the molecular heterogeneities (e.g., size and hydroxylation of acyl chains on the lipid A), this work is focused on the characterization of the different kinds of fatty acids subtituant of the di-GlcN backbone using low energy CID, thus allowing the competitive and eventually consecutive dissociations of acyl chains (i.e., when they are branched with other ester linkages) to be investigated. In addition, such MS^3 experiments of the singly charged species allow the localization of the fatty acids linked to the disaccharide ring skeleton. Furthermore, from the doubly deprotonated lipid A, submitted to collisions, it was possible to detect together the fatty acid anions and their complementary carbohydrate moieties. The main axis of this investigation was applied to the understanding of the fragmentation pathways involved in the dissociation of singly and doubly deprotonated lipid A molecules. Under low energy collision conditions, we focused on the chain cleavages that take place at a distance from the localized negative charge. We believe that, under such activation conditions, the deprotonated species decomposed by a stepwise process involving an isomerization into an ion–dipole complex prior to the dissociation. This mechanism was considered, in lieu of the charge-remote processes often proposed in the literature [22–24], to rationalize the observed decompositions (side chain releases as long chain ketene and long chain carboxylic acid neutrals).

1. Experimental

1.1. Chemicals and reagents

In this study, we focused on the lipid A extracted from the lipopolysaccharide from *Escherichia coli* J5 (Rc mutant). The LPS was purchased from Sigma–Aldrich Co. (St. Louis, MO, USA).

1.2. Sample preparation

The lipid A moieties were separately isolated from the crude LPS by mild acid hydrolysis according to a published protocol [25]. It consisted first in solubilizing in aqueous 0.02% triethylamine and adding acetic acid for a final concentration of 1.5% (v/v). Then, the mixture was heated at 100 °C during 2 h. After cooling, the lipid A was precipitated by addition of 1 M HCl for a final pH of 1.5. The insoluble analyte was centrifuged and washed with cold distilled water. Finally, the lipid A was obtained as a fluffy white solid after lyophilization.

The labeling experiment was performed with a mixture of $H_2{}^{18}O/H_2{}^{16}O$ (1/1, v/v), purchased from the CEA (Saclay, France). According to the protocol of acid hydrolysis, the LPS was solubilized in the latter solution instead of in water.

1.3. Electrospray ionization-ion trap mass spectrometry (ESI-ITMS)

Mass spectrometry experiments were performed in negative ion mode on an electrospray-ion trap instrument (Esquire 3000, Bruker-Franzen, Bremen, Germany). The lipid A was solubilized in chloroform/methanol (1/1, v/v) and diluted in pure methanol in order to obtain a final concentration of 20 pmol μL^{-1}. Then, the sample, was directly infused with a syringe pump, with a flow rate set to 3 $\mu L\,min^{-1}$. The nitrogen nebulization and drying gas (180 °C) were set to 5.4×10^4 Pa and 6 $L\,min^{-1}$, respectively. The mass spectrometry analyzes were operated with an electrospray capillary high voltage of 3.8 kV. The declustering potentials through the capillary exit (V_{CE}) and skimmer (V_{SK1}) voltages, as well as the trapping parameter through the low mass cut-off value (LMCO), are reported in each figure caption or detailed in the text. In order to perform the sequential MS^n experiments, each precursor ion was selected with an isolation width of 4 Th and was excited by resonant excitation voltage fixed between 0.6 $V_{p–p}$ and 1.6 $V_{p–p}$, according to the intensity of the parent ion signal. Data were acquired on an *m*/*z* range of 50–2000 Th with a scanning rate of 13000 Th s^{-1}. The mass spectra and CID spectra were the average of 20 scans.

2. Results and discussion

2.1. Influence of experimental ESI conditions on the observed deprotonated species

After the mild acid hydrolysis of *E. coli* LPS to recover the free lipid A, the influence of the MS instrument source

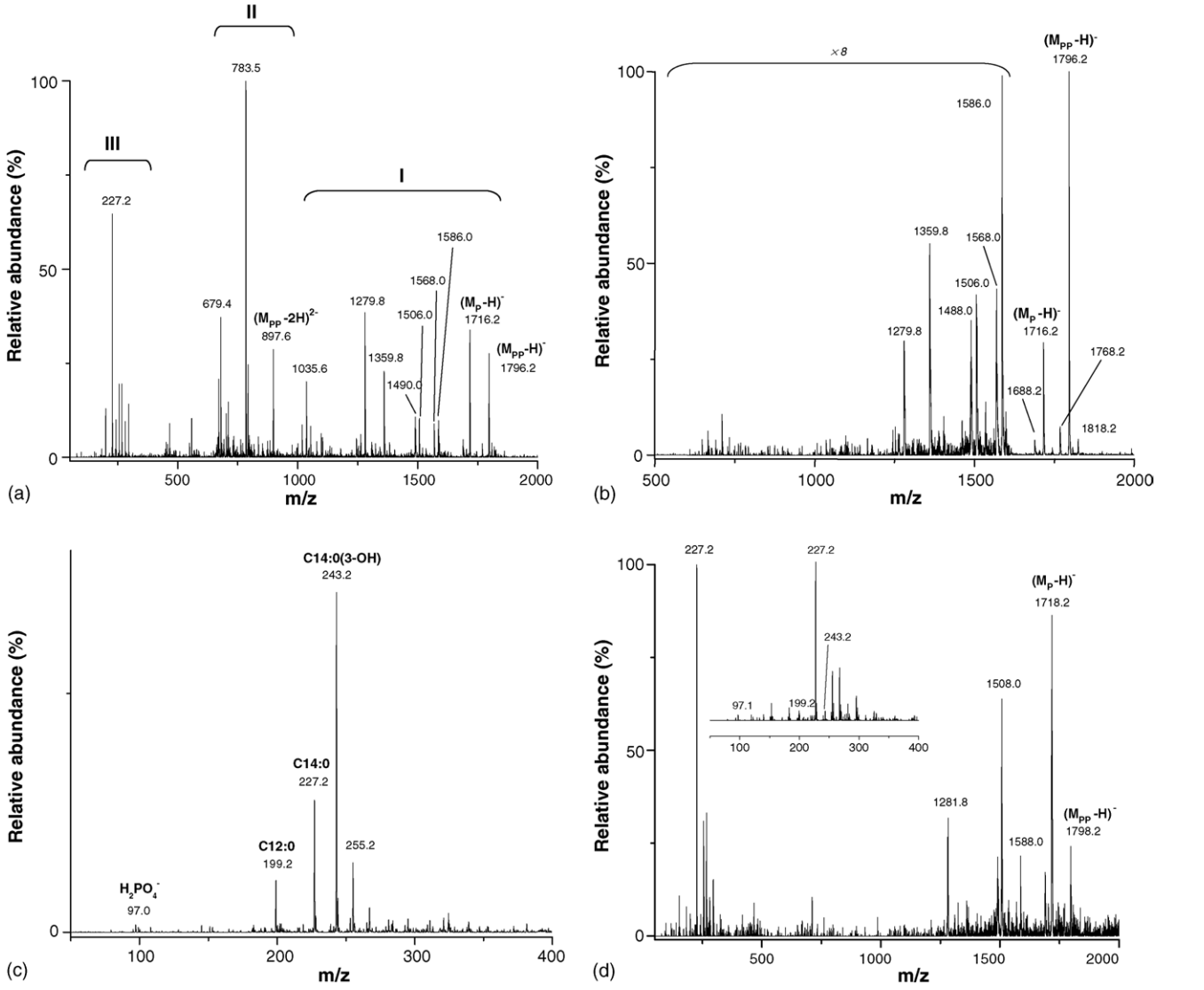

Fig. 1. Negative-ion ESI mass spectra of the diphosphoryl lipid A from *E. coli* J5 in the following conditions of in-source desolvation: (a) $V_{CE} = -190$ V, $V_{SK1} = -83$ V and LMCO = 67 Th, (b) $V_{CE} = -240$ V, $V_{SK1} = -100$ V and LMCO = 101 Th, (c) $V_{CE} = -140$ V, $V_{SK1} = -56$ V and LMCO = 31 Th and (d) after mild acid hydrolysis using $H_2{}^{18}O$ with $V_{CE} = -189$ V, $V_{SK1} = -83$ V and recording conditions LMCO = 101 Th (with M_P and M_{PP} corresponding to the mono and diphosphorylated lipid A, respectively).

conditions was investigated. Indeed, the analysis of the previously extracted diphosphoryl lipid A (DPLA) presents a complex fingerprint on the ESI mass spectrum (Fig. 1a). It can be divided into three dominant *m*/*z* zones corresponding to: (i) the upper *m*/*z* values, singly charged lipid A species (region I), (ii) the intermediate *m*/*z* values, doubly deprotonated lipid A (region II) and (iii) the lower *m*/*z* values, a distribution of free fatty acids (region III). In order to improve the signal of each zone of the whole scan width (50–2000 Th) the source and trapping parameters were optimized. In the following text, monophosphorylated species (MPLA) are noted as "M_P" and diphosphorylated species (DPLA) are noted as "M_{PP}" molecules.

2.2. Optimization of the higher m/z range of the mass spectrum: observation of deprotonated lipid A and various deacylated species (region I)

The upper *m*/*z* range (i.e., from 1000 to 1800 Th), displays anion species related to different singly deprotonated molecules with various acylation states (Fig. 1b). As the most abundant ions, the couple of hexaacylated species appear at *m*/*z* 1716.3 and *m*/*z* 1796.3, noted as $[M_P - H]^-$ and $[M_{PP} - H]^-$, respectively. The ESI mass spectrum displayed in Fig. 1b was recorded with rather (i) "hard desolvation conditions" ($V_{CE} = -240$ V, $V_{SK1} = -100$ V) and (ii) high LMCO value (i.e., 101 Th), in order to optimize the detection of the high mass-to-charge ratio ions.

With the exception of these two deprotonated species, various deacylated species are seen in on the ESI mass spectrum (amplified abundance area, see Fig. 1b). Especially, the ions at *m*/*z* 1586.0, *m*/*z* 1506.0, *m*/*z* 1359.8 and *m*/*z* 1279.8 which are assigned to $[(M_{PP}\text{-H})\text{-}C_{12}H_{25}CHCO]^-$, $[(M_P\text{-H})\text{-}C_{12}H_{25}CHCO]^-$, $[(M_{PP}\text{-H})\text{-}C_{12}H_{25}CHCO\text{-}C_{11}H_{23}CH(OH)CHCO]^-$ and $[(M_P\text{-H})\text{-}C_{12}H_{25}CHCO\text{-}C_{11}H_{23}CH(OH)CHCO]^-$ ions, respectively (see Table 1). At this stage, they may originate: (i) either from gas phase dissociation of naked deprotonated $[M_{PP} - H]^-$ and $[M_P - H]^-$ molecules (or solvated anion species), (ii) or from bimolecular hydrolysis (in solution or in the droplet) via tetravalent intermediate formation. A priori, the losses of the C_{14} alkyl ketenes from the C-3 and/or C-3′ positions of each glucosamine moiety from di- and monophosphorylated lipid A species could take place either competitively (i.e., leading to *m*/*z* 1586.0 and *m*/*z* 1506.0, respectively) or consecutively (i.e., *m*/*z* 1359.8 and *m*/*z* 1279.8, respectively). However, the contribution of various acylated lipids A produced from the natural lipopolysaccharide distribution (characterized by lower states of acylation and phosphorylation) could be considered also as precursor species. The former proposition has been ruled out because of absence of certain acylated chain releases in the CID spectra (vide infra). Thus, these side chain releases must take place in solution during the hydrolysis of the LPS and, in a second step, in the sample solution ($CHCl_3/CH_3OH$) or by dissociation of solvated deprotonated species at the skimmer [26].

Among the lower abundance molecular species, the *m*/*z* 1818.2 ion is assigned to the sodiated $[M_{PP} - 2H + Na]^-$ negative ion, whereas the *m*/*z* 1568.0 and *m*/*z* 1488.0 species are produced through ester bond cleavages (i.e., fatty acid release) occurring at the C-3 and C-3′ positions.

2.3. Optimization of the lower m/z range of the ESI mass spectrum: observation of free deprotonated fatty acids (region III)

By lowering significantly the LMCO value (from 81 to 31 Th), as well as decreasing the desolvation voltages, the fingerprint characterizing the low *m*/*z* range (i.e., from 200 to 400 Th) is enhanced (Fig. 1c). First, the expected $H_2PO_4^-$ and PO_3^- ions, respectively at *m*/*z* 97.0 and *m*/*z* 79.0, produced by the release of phosphate residue initially linked either at the C-1 or at the C-4′ position, were observed within very low abundances. This result suggests that the C–O–P bonds (located at the anomeric position or not) present a particularly high stability. These low *m*/*z* ion are assigned to deprotonated fatty acids which constitute the various acyl chains of the lipid A. Thus, the observed *m*/*z* 199.2, *m*/*z* 227.2 and *m*/*z* 243.2 ions are attributed to dodecanoate (i.e., C12:0), tetradecanoate (i.e., C14:0) and 3-hydroxydecanoate [i.e., C14:0(3-OH)] species, respectively. The most abundant ion (*m*/*z* 243.2), is attributed to the $C_{11}H_{22}CH(OH)CH_2CO_2^-$ carboxylate species produced through lipid A ester bond hydrolysis at the C-3 and/or C-3′ positions. These side chains are indeed particularly labile.

In order to confirm the origin of these carboxylate anions (i.e., ester hydrolysis either in solution or by gas phase dissociation of

Table 1
Structure of the various observed neutral side chain losses from dissociation of the singly and doubly charged lipid A species.

Implied chain (location)	Chemical nature of neutral losses	Chemical structure	Elemental formula	Mw[a]
C12:0	Alkyl ketene	$CH_3{-}(CH_2)_9{-}CH{=}C{=}O$	$C_{12}H_{22}O$	182.2
C-2′ (oxo)	Alkyl carboxylic acid	$CH_3{-}(CH_2)_{10}{-}COOH$	$C_{12}H_{24}O_2$	200.2
C14:0	Alkyl ketene	$CH_3{-}(CH_2)_{11}{-}CH{=}C{=}O$	$C_{14}H_{26}O$	210.2
C-3′ (oxo)	Alkyl carboxylic acid	$CH_3{-}(CH_2)_{12}{-}COOH$	$C_{14}H_{28}O_2$	228.2
C14:0(3-OH)	3-Hydroxylated alkyl ketene	$CH_3{-}(CH_2)_{10}{-}CH(OH){-}CH{=}C{=}O$	$C_{14}H_{26}O_2$	226.2
C-3 et/ou C-3′	3-Hydroxylated alkyl carboxylic acid	$CH_3{-}(CH_2)_{10}{-}CH(OH){-}CH_2{-}COOH$	$C_{14}H_{28}O_3$	244.2
C14:0(3-OH)	Unsaturated alkyl ketene	$CH_3{-}(CH_2)_9{-}CH{=}CH{-}CH{=}C{=}O$	$C_{14}H_{24}O$	208.2
C-3′	Unsaturated alkyl carboxylic acid	$CH_3{-}(CH_2)_{10}{-}CH{=}CH{-}COOH$	$C_{14}H_{26}O_2$	226.2
C14:0[3-O(C14:0)] C-3′	Alkyl-oxo-alkyl ketene	$CH_3{-}(CH_2)_{10}{-}CH(O{-}[C14:0]){-}CH{=}C{=}O$	$C_{28}H_{52}O_3$	436.4

[a] Monoisotopic molecular weight.

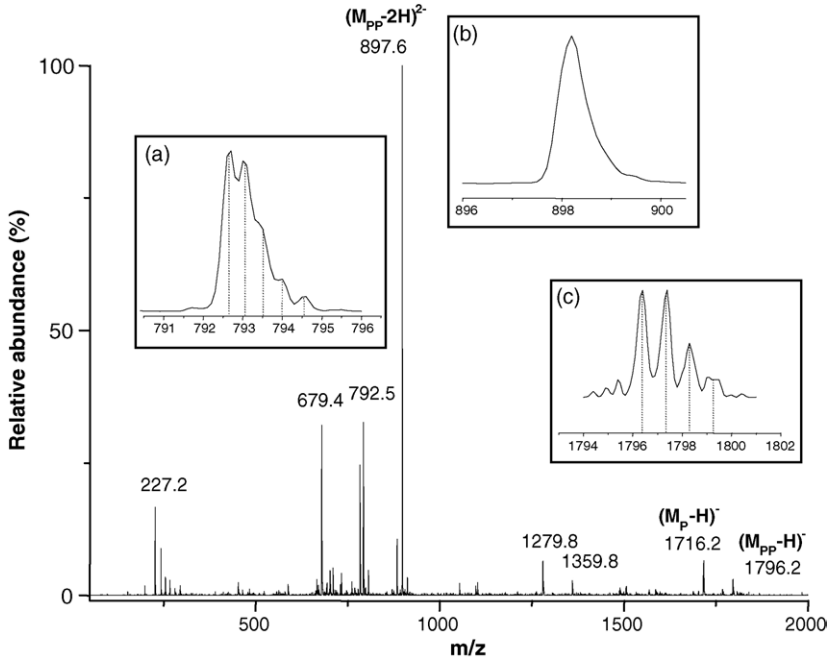

Fig. 2. Negative-ion ESI mass spectrum of the diphosphoryl lipid A from *E. coli* acquired under soft desolvation conditions (with M_P and M_{PP} corresponding to the mono and diphosphorylated lipid A, respectively). In the inserts are represented ions at (a) *m/z* 792.5, (b) *m/z* 897.6 and (c) *m/z* 1796.2. (Conditions of in-source desolvation: $V_{CE} = -140$ V, $V_{SK1} = -56$ V and LMCO = 67 Th.)

solvated anions), an experiment based upon isotopic ^{18}O labeling was performed during the crude LPS hydrolysis using an acidified $H_2{}^{18}O/H_2{}^{16}O$ (1/1) mixture. The ESI mass spectrum of the $^{18}O/^{16}O$ labeled sample (Fig. 1d) displays a 2 Th shift of all the high *m/z* ions. It is assigned to the heaxaacylated deprotonated molecules which appear at *m/z* 1798.2 and *m/z* 1718.2, as well as the deacylated derived species which are shifted at *m/z* 1588.0, *m/z* 1508.0 and *m/z* 1281.8. Alternatively, the various ^{18}O labeled forms of lipid A ions do not generate deprotonated ^{18}O labeled fatty acids (i.e., *m/z* 199.2, *m/z* 227.2 and *m/z* 243.2) confirming that the observed fatty acid anions are not produced during the preliminary hydrolysis step, but seem to be induced later during "in source" dissociations of solvated deprotonated species. Actually, the labeling was introduced at the Kdo/GlcN linkage by $H_2{}^{18}O/H+$ hydrolysis, i.e., at the primary alcohol at the C-6′ position.

2.4. Optimization at medium m/z values of mass spectrum: discrimination of the single charged species in favor of doubly charged species (region II)

The charge-state distribution depends on the desolvation and trapping conditions (i.e., the LMCO value) and mainly favors doubly deprotonated lipid A molecules; are favored with softer desolvation conditions (i.e., voltages applied to the capillary exit and to the skimmers were $V_{CE} = -190$ V, $V_{SK1} = -83$ V, respectively). In the gas phase, the phosphate groups being the lipids A most acidic sites [21], a distant double deprotonation can occur regioselectively on these sites to give rise to the formation of the doubly charged $[M_{PP} - 2H]^{2-}$ lipid A (i.e., *m/z* 897.6), as displayed in the ESI mass spectrum (Fig. 2). Under these experimental conditions, the doubly deprotonated $[M_{PP} - 2H]^{2-}$ species are at *m/z* 897.6, the base peak. In addition, other doubly charged ions can be observed at *m/z* 792.5 and *m/z* 679.4 corresponding to hexaacylated $[(M_{PP}\text{-}2H)\text{-}C_{12}H_{25}CHCO]^{2-}$ and pentaacylated $[(M_{PP}\text{-}2H)\text{-}C_{12}H_{25}CHCO\text{-}C_{11}H_{23}CH(OH)CHCO]^{2-}$ lipid A species, respectively.

The lack of resolution for the signal at *m/z* 897.6 as compared to the *m/z* 792.5 ion can be explained by considering that this doubly charged ion is somewhat unstable and may decompose promptly by application of the axial modulation during the analytical scan [27–30] into the ion trap analyzer.

The increase of the voltage offset between the capillary exit and the skimmer yields a change in relative abundances of the doubly charged ions as shown in Fig. 3, mainly, the abundance of the doubly deprotonated *m/z* 897.6 lipid A decreases significantly to become lower than that of the corresponding doubly charged *m/z* 792.5 ion obtained by losing a C_{14} side chain. Thus confirming that it was produced by "in source" dissociation rather than by an initial hydrolysis in solution. In addition higher capillary exit-skimmer voltage differences lead to the increase of the singly charged ions relative abundance as compared to the doubly charged species.

This change in relative abundance between singly and doubly charged ions is attributed to: (i) harder desolvation conditions and/or, (ii) to an *m/z* discrimination in favor of higher *m/z* ratios by increase of the voltage offset (better transmission of the higher *m/z* ions). Nevertheless, the latter discrimination origin should be moderated. Indeed, such discrimination should be unfavorable

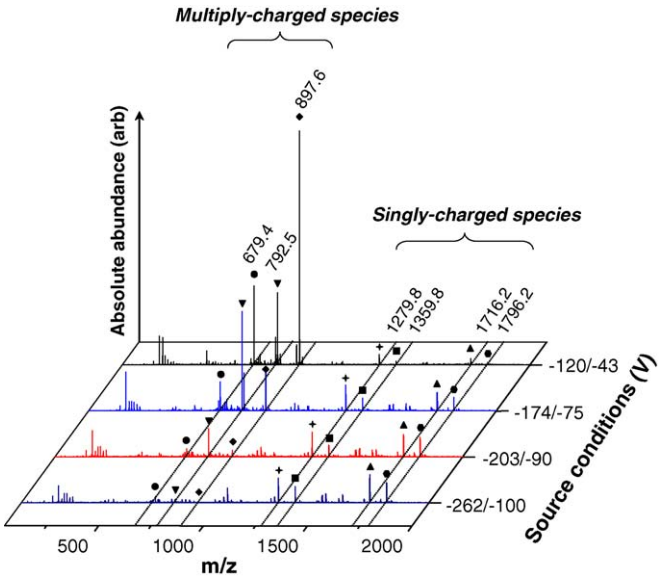

Fig. 3. Effect of the source voltages (V_{CE}/V_{SK1} in volts) applied to the desolvation chamber on the various charge-state distribution of ions in ESI mass spectra (LMCO = 67 Th).

to the observation of deprotonated fatty acids (*m/z* lower than 300 Th) which was not the case.

2.5. Fragmentation orientation of various molecular species under low energy CID conditions

Several studies on the deprotonated lipid A dissociations have been carried out under low energy collision conditions [19,20,23]. Charge-remote processes [31,32] are mainly proposed [22,24,33] in order to rationalize the observed neutral side chain losses, although the negative charged was not adjacent to the cleavage bond. However, such a mechanism should be unfavored under low energy excitation conditions [34]. Indeed, charge-remote processes must involve in particular electronic level excitation allowing radical intermediate species formation as it occurs with high energy collision conditions (e.g., from deprotonated fatty acids and analogous species). Comparison between high energy versus low energy collision conditions was developed [34] a long time ago and have demonstrated the influence of the internal energy of excited ions as well as the kinetic shift of the dissociation processes on the charge-remote mechanism. This effect is reinforced by the high activation energy required for such reactions. From these kinetic properties, it is expected that such charge-remote mechanisms must be strongly unfavorable under low energy CID conditions, especially using an ion trap analyzer.

In order to propose an alternative mechanism involving charge-driven processes to explain this behavior, we reinvestigated dissociations of singly $[M_{PP} - H]^-$ {and $[M_P - H]^-$} and doubly deprotonated $[M_{PP} - 2H]^{2-}$ anions. Moreover, the comparison of the gas phase dissociations could determine the direct influence of the phosphate groups on the fragmentation orientation. The various observed losses generated under low energy collision conditions are summarized in the Table 1.

2.6. Dissociation of singly charged species under low energy collision conditions

2.6.1. Behavior of monophosphated species $[M_P - H]^-$

The monophosphorylated species are produced by hydrolysis of the phosphate group occuring by nucleophilic attack at the phosphate site as shown in Scheme 2. In this mechanism, the oxygen atom linked to the C-1 position is non labile during the phosphoryl group release and thus, the incorporation of ^{18}O at this position cannot occur, inducing its introduction into the phosphoric acid at the C-4′ position. The mechanism proposed (Scheme 2) is known to be favored from the anomeric position (i.e., the C-1 position) because of the presence of the oxygen atom in the sugar ring. If we take this into consideration, it is expected that the phosphate at C-1 will be a very good leaving group as compared to the phosphate at C-4′ which is less activated since no electron-withdrawing group is present.

As shown in the CID spectrum of $[M_P - H]^-$ (Fig. 4), the negative charge located at the phosphate group may promote major cleavage processes involving competitive eliminations of fatty acid residues (see Table 1) from:

(i) the branched positions either at C-2′ yielding loss of the C12:0 chain (-200 u) to give rise to formation of the product ion at *m/z* 1516.1 or at the C-3′ position generating the *m/z* 1488.0 ion by neutral loss of the 228 u (i.e., the C14:0 fatty acid chain) as the major pathway;
(ii) the ester at C-3 position by neutral elimination of the 244 u [i.e., the C14:0(3-OH) fatty acid loss] yielding the *m/z* 1472.0 product ion with a lower abundance.

From each product ions of the first generation, consecutive dissociations take place by elimination of alkyl carboxylic acid or alkyl ketene neutrals (Table 1). For instance, from the major

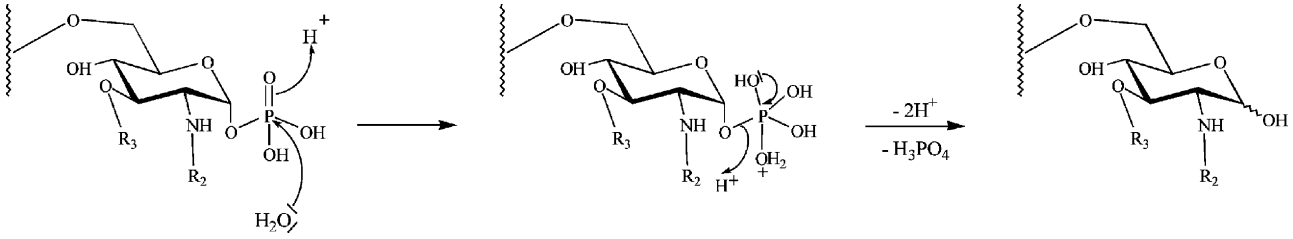

Scheme 2. Proposed mechanism for the dephosphorylation reaction at the anomeric position e.g., in acid hydrolysis conditions.

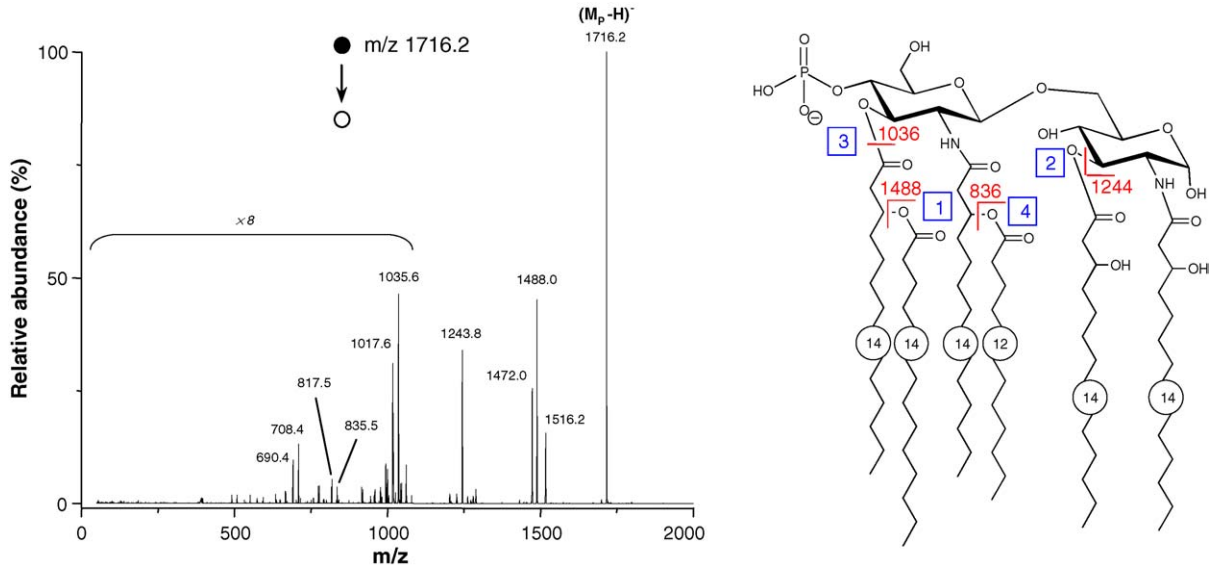

Fig. 4. Low energy CID mass spectrum of the monophosphorylated specie $[M_P - H]^-$ at m/z 1716.2 and proposed formal cleavage of major competitive fragmentations of the parent ion. (Conditions of in-source desolvation: $V_{CE} = -140$ V, $V_{SK1} = -56$ V, LMCO = 67 Th, MS/MS conditions: isolation width = 4 u and fragmentation amplitude = 0.8 V_{P-P}). (The numbers included into squares are associated to the dissociation order.)

product ion at m/z 1488.0, the carboxylic acid C14:0(3-OH) neutral (−244 u) can be released by ester bond cleavage of the hydroxyl ester group at C-3 position yielding m/z 1243.8. This latter ion decomposed further to give the m/z 1035.6 ion through the elimination of the unsaturated alkyl ketene neutral (208 u loss) from the residual branched ester at the C-3′ position. These eliminations are confirmed by the sequential MS^3 experiments from the product ions at m/z 1488.0 and m/z 1243.8 generated from the m/z 1488 precursor ion (Table 2, Fig. 5a and c). It should be pointed out that the complementary carboxylate ions (i.e., in the range 200–300 Th) cannot be displayed in the CID spectrum of m/z 1716.2 because of the low mass cut-off discrimination (i.e., only product ion with m/z that are at least equal to the quarter of the parent ion m/z can be usually detected).

Interestingly, the m/z 1472.0 product ion, obtained via the carboxylic acid C14:0(3-OH) release, is able to give rise consecutively to m/z 1243.8 by the loss of the C14:0 fatty acid neutral (−228 u) (Fig. 5b). The m/z 1243.8 product ion can also be produced from the consecutive dissociation of the m/z 1488.0 product ion (Table 2). The m/z 1287.9 and m/z 1271.9 product ions produced consecutively from m/z 1716.2 are formed by elimination of the 228 and 244 u neutral, respectively. These neutrals are the C14:0 and C14:0(3-OH) fatty acids coming from the intact C-3′ and C-3 positions, respectively.

To rationalize these dissociations without involving charge-remote processes, other mechanisms can be proposed as alternative (Scheme 3). They will allow rationalizing the observed fragmentations by considering charge-driven cleavages through stepwise pathways resulting in fatty acids or long chain alkyl ketenes releases. These mechanisms are based upon precursor ion isomerization into ion–dipole complexes [35] prior to dissociation of the deprotonated mono-phosphorylated molecule (as well as in the case of diphosphorylated lipid A, vide infra).

Table 2
Synthesis of product ions recovered after MS^n experiments

Second generation parent ions (MS^3)	Product ions (percent relative abundance)
1796 → 1698	1680 (3.4), 1470 (100), 1454 (8.7), 1244 (34.3), 1226 (5.6), 1036 (6.5), 1018 (3.4), 1000 (2.5)
1796 → 1568	1550 (35.6), 1470 (43.7), 1324 (100), 1244 (18.4), 1226 (47.1)
1796 → 1552	1534 (31.3), 1454 (100), 1352 (90.6), 1226 (64.0)
1796 → 1470	1262 (7.9), 1244 (63.2), 1226 (100)
1796 → 1454	1436 (9.9), 1352 (100), 1226 (98.8), 1018 (13.3), 1000 (7.3)
1796 → 1244	1036 (100), 1018 (54.0)
1796 → 1226	1208 (49.6), 1018 (100), 1000 (35.2)
1796 → 1036	1018 (59.3), 1000 (49.2), 835 (100)
1716 → 1516	1288 (1001 1270 (68.9)
1716 → 1488	1470 (5.0), 1244 (100), 1226 (6.3), 1036 (0.9), 1018 (1.7), 1000 (1.5)
1716 → 1472	1244 (100), 1036 (3.4), 1018 (13.1)
1716 → 1244	1226 (13.3), 1036 (100) 1018 (63.2), 835 (3.2), 817 (2.0)
1716 → 1036	835 (100)

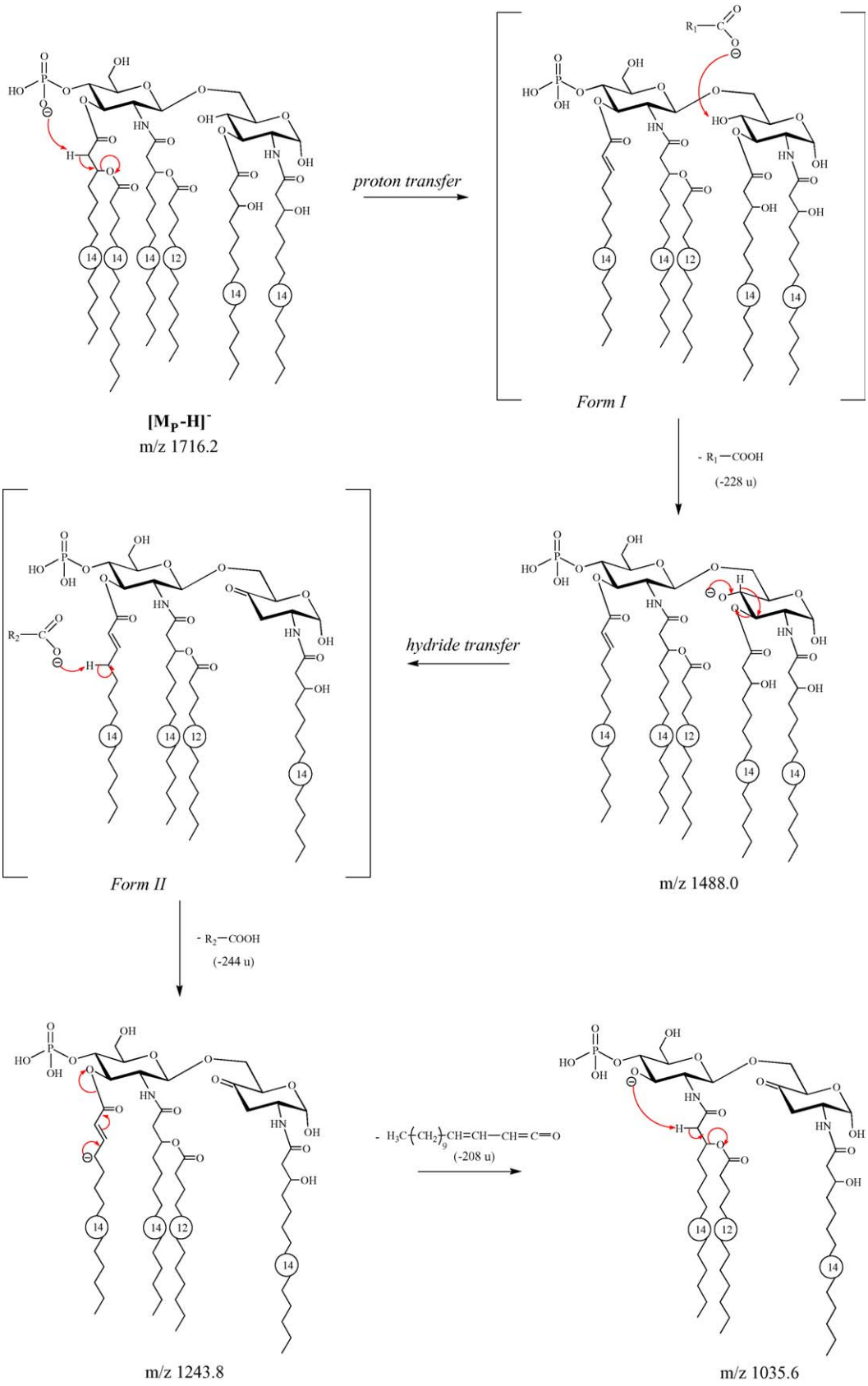

Scheme 3. Major consecutive fragmentation pathways resulting from the monophosphated $[M_P - H]^-$ species via ion–dipole formation involved in the stepwise fragmentations occurring under low energy collision conditions (the fatty acyl chains lost above were defined as $R_1 = CH_3\text{-}(CH_2)_{12}\text{-}$, $R_2 = CH_3\text{-}(CH_2)_{10}\text{-}CH(OH)\text{-}CH_2\text{-}$, $R_3 = CH_3\text{-}(CH_2)_{10}\text{-}$).

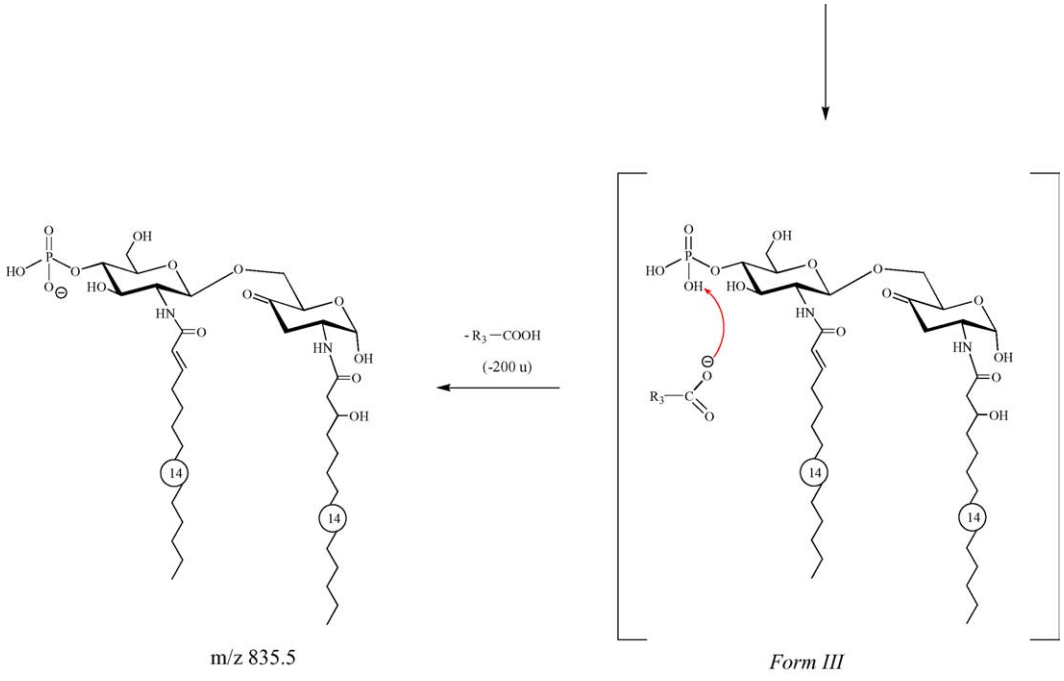

Scheme 3. (*Continued*).

Such isomerization was first introduced to explain long distance charge migration occurring from the dissociation of odd-electron species [36], for positive even-electron ions and latter for negative ions. From even-electron anions, the production of ion–dipole complexes by simple bond cleavages allowed to favor inter-partner proton transfer, independently of the initial charge location. This isomerization is induced by the phosphate groups, considered as a weak basic site, which may remove, under CID conditions, a proton from an acidic site at the α-position of the branched ester linked at the C-3′ position, generating an α–β elimination leading to an ion–dipole complex (form I). The carboxylate partner can remove proton competitively from various acidic sites such as:

(i) phosphate group at C-4′,
(ii) enolizable α-position of various esters (or unlikely amides),
(iii) secondary alcohol at the C-1 or C-4 position of the neutral partner of the binary complex.

Such an internal proton transfer led to the C14:0 fatty acid release (loss of 228 u), yielding the *m*/*z* 1488.0 product ion after ion-dipole dissociation. Sequential MS^3 experiments on the *m*/*z* 1488.0 ion (*m*/*z* 1716 → *m*/*z* 1488 →) led to the product ion at *m*/*z* 1243.8 as major second generation species, which can be rationalized by considering the particular reactivity of the secondary alkoxy group at the C-4 position (Scheme 3). This alkoxy group is able to reduce the C–O bond by an 1-2 hydride transfer, leading to, the hydroxycarboxylate anion release occurs from the C-3 position leading to a new ion–dipole complex (form II). The carboxylate can remove a proton from various acidic site (as described previously) and especially from the allylic position of the produced unsaturated ester side chain linked to the C-3′ position. From this intra ion–dipole proton transfer, the hydroxy fatty acid (244 u) can be lost to give rise to the *m*/*z* 1243.8 product ion. The conjugated carbanion on the ester side chain (C-3′ position) promotes the direct O–CO bond cleavage by the unsaturated ketene release (loss of 208 u neutral) generating the *m*/*z* 1035.6 product ion. Finally, the obtained alkoxy at C-4′ position may induce an α–β elimination of the C12:0 side chain by a proton transfer yielding a new ion–dipole complex (form III). This ion–dipole yields the C12:0 fatty acid release by a second proton transfer from one acid site (i.e., a phosphate group) to give rise to the *m*/*z* 835.5 product ion in which only the amide bonds were preserved. Interestingly, this discussion shows how by using either the flexibility of the ester (or amide) side chains or the ion–dipole complex formation it is possible to favor distant proton transfer through internal charge solvation as well as "charge relay" processes [37] (useful for the stepwise multiple proton transfers). The produced elimination involves carboxylic acid or ketene loss but no amide (or ketene from amide) which is not a good leaving group. All these proposed competitive and consecutive dissociations have been confirmed by performing sequential MS^3 and MS^4 experiments. Similar stepwise charge-driven dissociation via the formation of ion–dipole complexes can be proposed for explaining the behavior of the low abundant *m*/*z* 1488.0 and *m*/*z* 1516.1 ions in the sequential MS^3 experiments (Table 2). The latter ion (*m*/*z* 1516.1) is produced from the decomposition of the *m*/*z* 1716.2 ion (loss of 200 u from the ester at C-2′ position) and dissociate consecutively leading to (sequential MS^3 experiment, see Table 2) *m*/*z* 1287.9 (loss of 228 u) and *m*/*z* 1271.9 (loss of 244 u) ions, through losses of C14:0 at C-3′ and C14:0(3-OH) at the C-3 position monophosphorylated lipid A, respectively.

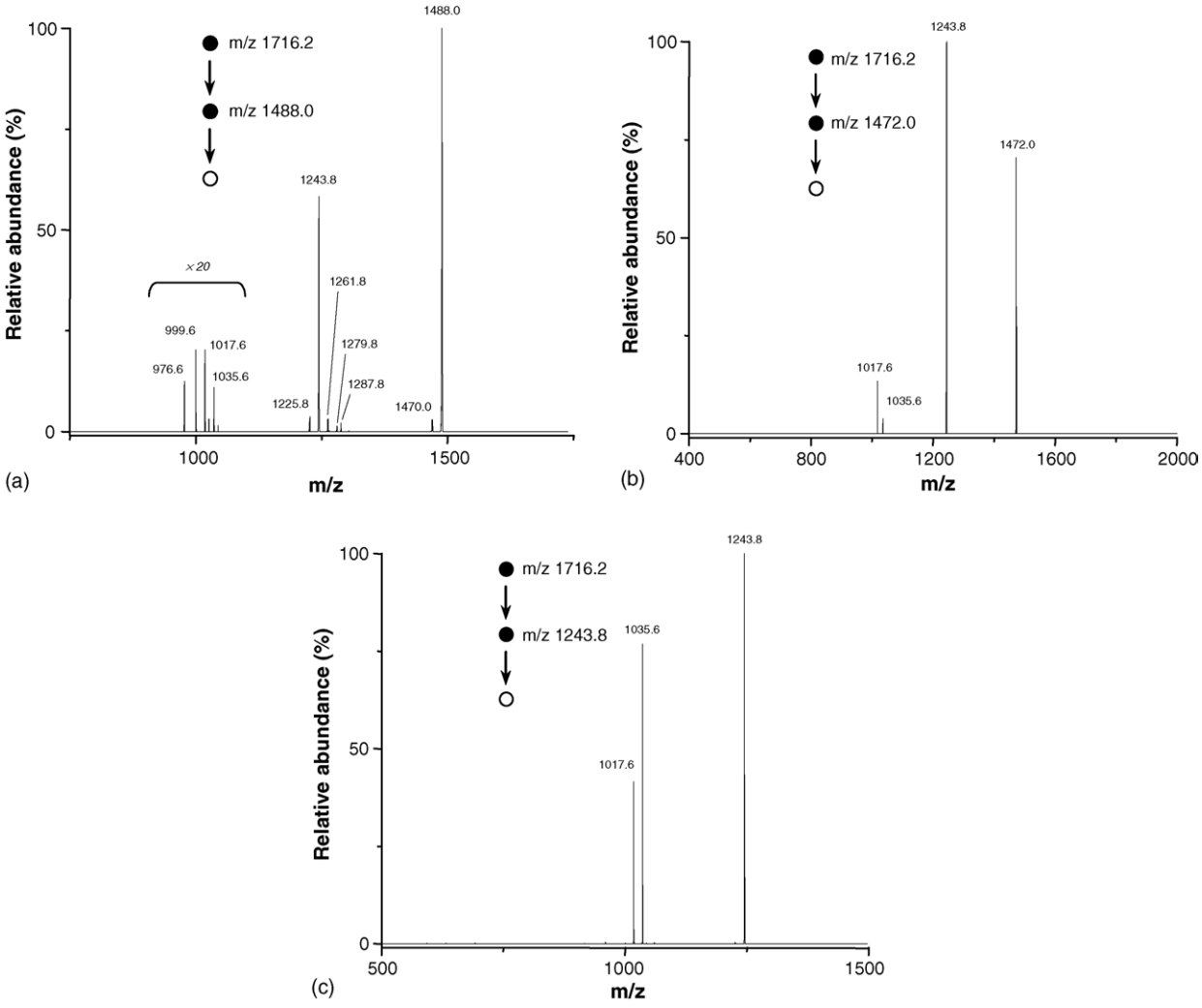

Fig. 5. ESI-MS^n mass spectra acquired from the monophosphorylated $[M_P - H]^-$ parent ion at m/z 1716.2 (Conditions of in-source desolvation: $V_{CE} = -140$ V, $V_{SK1} = -56$ V, LMCO = 67 Th, MS/MS conditions: isolation width = 4 u and fragmentation amplitude = 0.8 V_{P-P}), with: (a), MS^3 of m/z 1488.0 ion (isolation width = 4 u and fragmentation amplitude = 0.45 V_{P-P}), (b), MS^3 of m/z 1472.0 ion (isolation width = 4 u and fragmentation amplitude = 0.5 V_{P-P}) and (c), MS^3 of m/z 1243.8 ion (isolation width = 4 u and fragmentation amplitude = 0.6 V_{P-P}).

Note, the particular stability of the phosphate group at the C-4′ position of the monophosphorylated $[M_P - H]^-$ anion which is never directly released from both the first and second generations of product ions under these low energy CID conditions. In fact, the presence of the phosphate group is likely to allow maintaining the charge on the carbohydrate skeleton. Furthermore, it can be used as a relay for internal charge migration.

2.6.2. *Behavior of diphosphated $[M_{PP} - H]^-$ species*

By analogy to the previous mechanistic discussion, it is possible to rationalize dissociations of the $[M_{PP} - H]^-$ ion (m/z 1796.2) under low energy collision conditions (see Fig. 6). The recorded CID spectrum displays several product ions generated by competitive and/or consecutive decompositions. The dissociative pathways are promoted by the negative charge located on the phosphate group either at the C-1 or at the C-4′ position. The first generation of product ions are formed by the loss of the phosphate group (98 u) from the weak anomeric C-1 position of the $[M_{PP} - H]^-$ ion (vide supra) to give rise to the m/z 1698.2 product ion (Fig. 6). This process competes with the direct loss of fatty acids such as C12:0 (200 u), C14:0 (228 u) and C14:0(3-OH) (244 u) yielding the first generation of product ions at m/z 1596.0, m/z 1568.0 and m/z 1552.0, respectively. The latter is the major species resulting from the loss of hydroxy fatty acid at the C-3 position, close to the hydroxyl group (C-4 position) which is able to be deprotonated and yield the loss of C14:0(3-OH), by a stepwise process (1-2 hydride transfer). The minor species at m/z 1596.0 and m/z 1568.0 are produced through fatty acid losses (i.e., C12:0 and C14:0) from the branched side chains at the C-2′ and C-3′ positions, respectively. It should be pointed out that the HPO_3 loss (−80 u, less than 1%) from the doubly phosphorylated species {i.e., $[M_{PP} - H]^-$} is not observed. This contrasts with the loss of 98 u occurring from the anomeric position to give m/z 1698.2. Consecutively to the H_3PO_4 loss, the C14:0 fatty acid release takes place from the branched fatty acid at C-3′ to yield the m/z 1470.0 product ion (loss of 228 u), as confirmed by the sequential MS^3 experiments (Table 2, Fig. 7a). From the latter ion, a series of consecutive losses occurred leading to the

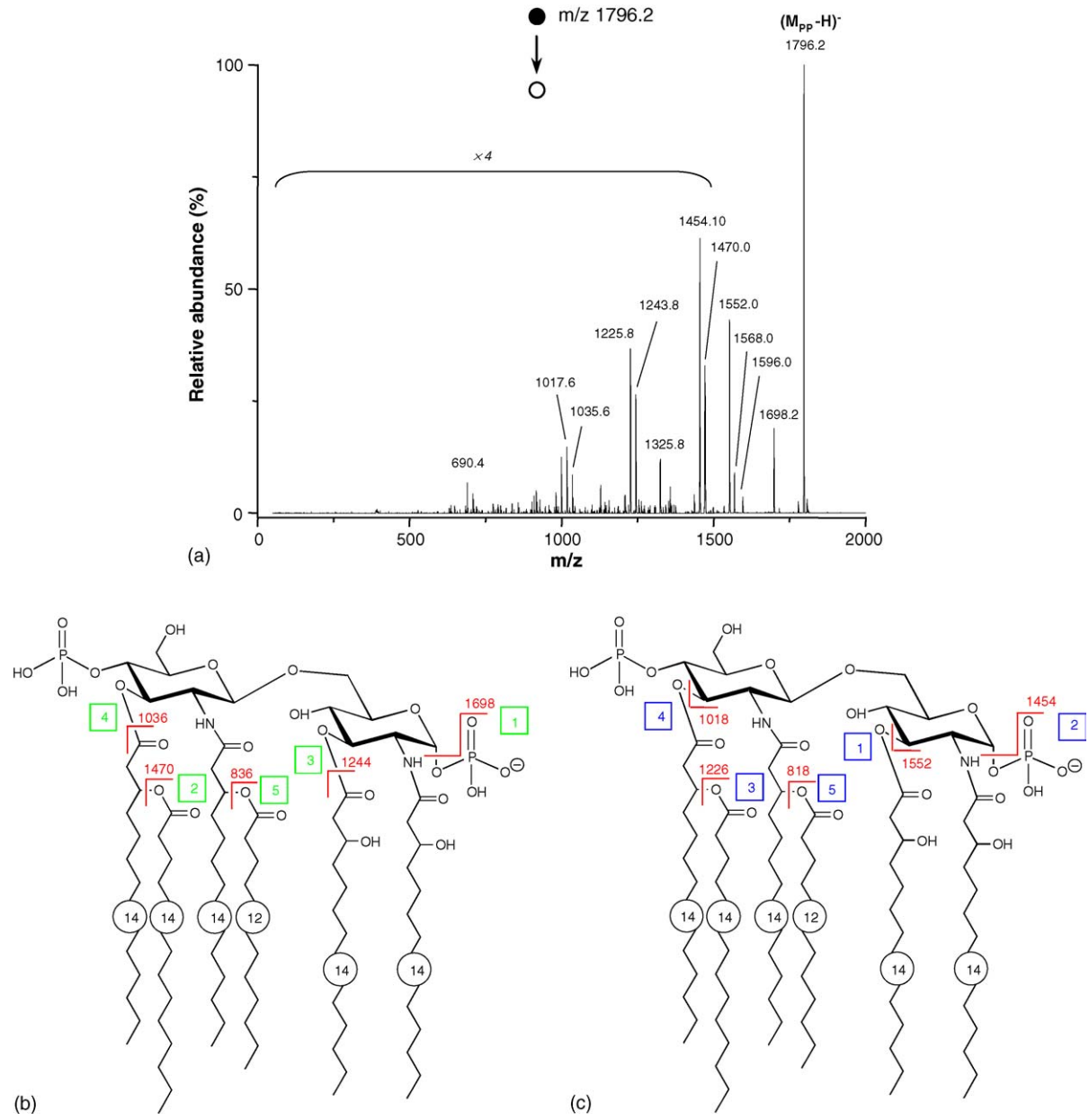

Fig. 6. (a) Low energy CID spectrum of the diphosphorylated $[M_{PP} - H]^-$ species at m/z 1796.2 (conditions of in-source desolvation: $V_{CE} = -140$ V, $V_{SK1} = -56$ V and LMCO = 67 Th, MS/MS conditions: isolation width = 4 u and fragmentation amplitude = 0.95 V_{P-P}), associated to proposed competitive and consecutive fragmentations of the selected m/z 1796.2 ion under low collision energy conditions, according to the first cleavage step: (b) either by loss of the anomeric phosphate or (c) by loss of the C14:0(3-OH) linked at the C-3 position. (The numbers included into squares are associated to the dissociation order.)

m/z 1243.8, m/z 1035.6 and m/z 835.5 product ions due to the release of 226 u, [226 + 208] u and [226 + 208 + 200] u, respectively (Fig. 6b and Table 2). In addition, the m/z 1552.0 ion led to the m/z 1454.0 ion through the loss of 98 u (phosphoric acid). Consecutively, other losses of side chains are considered and led to formation of the m/z 1225.8, m/z 1017.6 and m/z 817.5 product ions (Figs. 6c, 7b and c). These ions are similar to the stepwise pathway previously described from the m/z 1470.0 ion.

The mechanistic interpretation of these competitive and consecutive dissociations can be generated, as previously discussed, from the precursor $[M_P - H]^-$ ion via the formation of ion–dipole complexes. Among the two observed dissociation pathways involving (i) an initial loss of phosphate and (ii) an initial loss of fatty acid, only the first case will be detailed in the following discussion. For instance, from the dissociation initiated by the anomeric phosphoric acid neutral loss, a stepwise process firstly requires a migration of one proton from the neighboring hydroxylic group (substituting the acyl chain linked to the C-2 position) to the phosphate group (Scheme 4). The produced secondary alkoxy group promotes the C–OP(O) bond cleavage by hydride transfer. This reduction yields the phosphate ($H_2PO_4^-$) release which is involved in the formation of an ion–dipole complex (form I′). In a second step, a proton transfer occurs from the enolizable ester (linked to the C-3′ position) to this free phosphate anion. Then, the neutral H_3PO_4 can be removed from the complex to yield the m/z 1698.2 product ion.

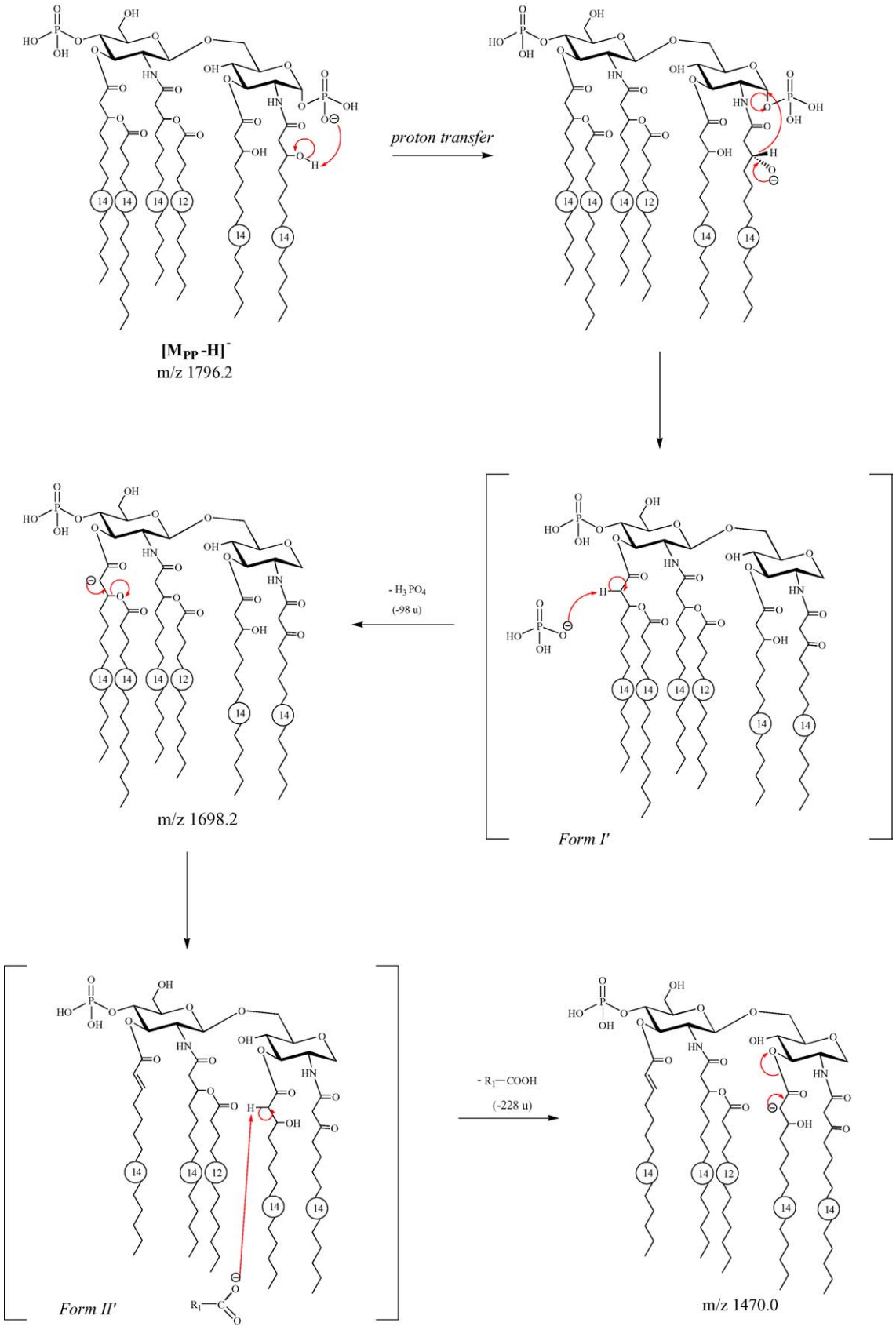

Scheme 4. Major consecutive fragmentation pathway from the monophosphated $[M_{PP} - H]^-$ species (the fatty acyl chains lost above were defined as $R_1 = CH_3$-$(CH_2)_{12}$-, $R_2 = CH_3$-$(CH_2)_{10}$-).

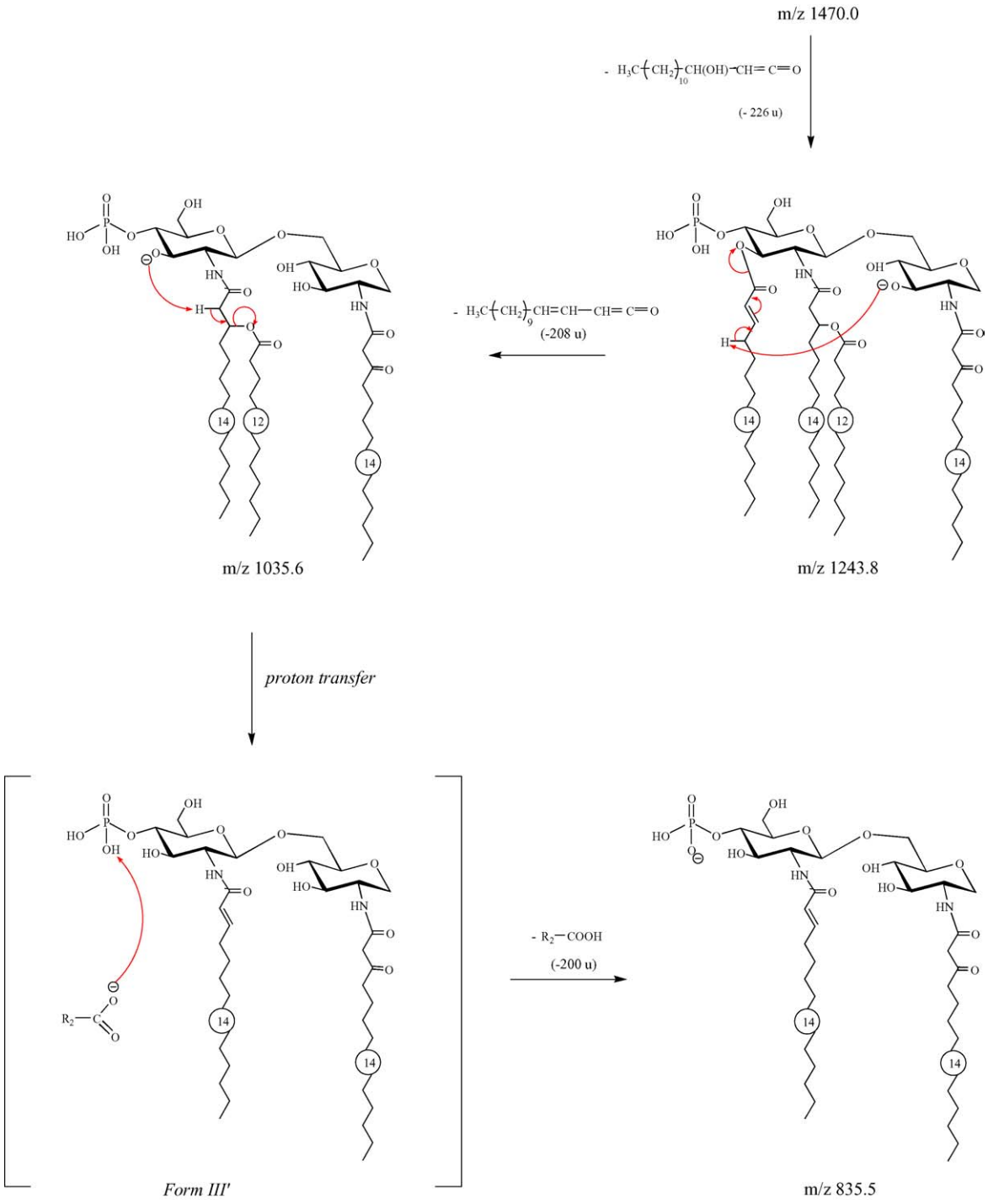

Scheme 4. (*Continued*).

The carbanion, present on the side chain, induces the α-cleavage in order to release the deprotonated C14:0 fatty acid solvated by the substituted disaccharide skeleton (ion–dipole, form II′). Prior to the direct cleavage, the carboxylate ion removes a proton from an acidic site. For instance, deprotonation can occur at the carbonyl group α-position of the ester chain linked to the C-3 position inducing the loss of the C14:0 fatty acid and the production of the *m*/*z* 1470.0 ion (Fig. 7a). This ion can dissociate by alkyl ketene release (−226 u) from the C-3 position by a charge-driven cleavage to generate the *m*/*z* 1243.8 product ion (Fig. 7b). The alkoxy site on this ion is able to receive a proton from an acidic site, especially from the α-position of the unsaturated ester linked to the C-3′ position. In this way the unsaturated ketene release (loss of 208 u) occurs leading to the *m*/*z* 1035.6 ion. Then, from this *m*/*z* 1035.6 product ion, the deprotonation at the amide α-position linked to the C-2′ carbon induces the α-cleavage and the release of the deprotonated C12:0 fatty acid (ion–dipole, form III′). Finally, the carboxylate ion removes a

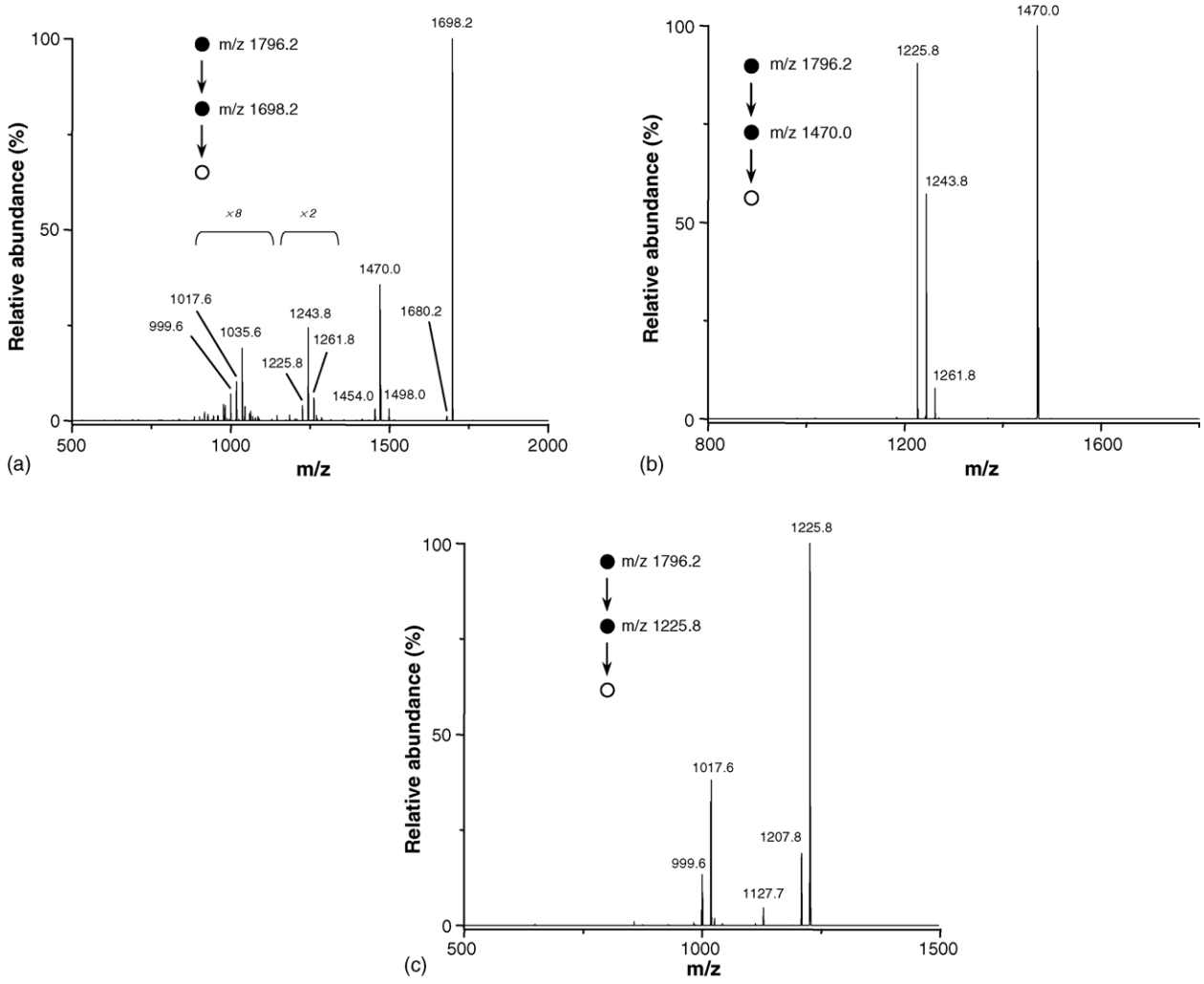

Fig. 7. ESI-MS^n mass spectra acquired from the diphosphorylated $[M_{PP} - H]^-$ parent ion at m/z 1796.2 (Conditions of in-source desolvation: $V_{CE} = -140$ V, $V_{SK1} = -56$ V, LMCO = 67 Th, MS/MS conditions: isolation width = 4 u and fragmentation amplitude = 0.95 V_{P-P}), with: (a), MS^3 of m/z 1698.2 ion (isolation width = 4 u and fragmentation amplitude = 0.85 V_{P-P}), (b), MS^3 of m/z 1470.0 ion (isolation width = 4 u and fragmentation amplitude = 0.48 V_{P-P}) and (c), MS^3 of m/z 1225.8 ion (isolation width = 4 u and fragmentation amplitude = 0.46 V_{P-P}).

proton from an acidic site (i.e., easily from the phosphate group) leading to the loss of the C12:0 neutral chain (carboxylic acid) yielding the m/z 835.5 product ion (Scheme 4).

2.7. Dissociation of doubly charged species

The study under low energy collision conditions of the $[M_{PP} - 2H]^{2-}$ ion (m/z 897.6) resulted in various singly and doubly charged product ions (Fig. 8). Doubly charged product ions are observed at m/z 783.5, corresponding to the loss of the branched acyl chain in the C-3′ position (−228 u) and, to a lesser extent, to the m/z 679.4 ion corresponding to the consecutive loss of the acyl chain in the C-3′ position (−208 u). Note the presence, as a minor species, of the ion at m/z 797.6 produced by the dissociation of the C12:0 acyl chain linked to the C-2′ carbon. In addition, the CID spectrum of the m/z 897.6 ion displayed the formation of several singly charged product ions (Fig. 8a). The ions at m/z 1796.2 and 1716.2 corresponds to $[M_{PP} - H]^-$ and to the loss of PO_3^- (m/z 79), respectively, while the product ion at m/z 1552.0 is due to the release of the acyl chain at the C-3 position (−244 u). The m/z 1568.0 singly charged ion is equivalent to the doubly deprotonated m/z 783.5 product ion. The ion at m/z 1488.0 is produced through the consecutive loss of the branched acyl chain in the C-3′ position (−228 u) from the m/z 1716.2 ion. The minor ion at m/z 1359.8 is the singly charged species corresponding to the doubly charged m/z 679.4 product ion. The low abundance ions at m/z 1243.8 and m/z 1287.8 are produced consecutively from the m/z 1488.0 ion with neutral acyl chain losses of 244 u,(chain linked in the C-3 position) and 200 u (chain branched in C-2′ position). The ions observed at m/z 1323.8 and 1343.8 correspond to competitive side chain cleavages at C-3 and C-3′ positions, respectively, from the m/z 1568.0 ion. The CID experiments of the doubly charged species, enabled the trapping of the low m/z ions. Thus, the m/z 243.1 ion displayed on the Fig. 8a corresponds to the hydroxymyristate species [C14:0(3-OH)]. Moreover, the MS^3 analysis of the ion

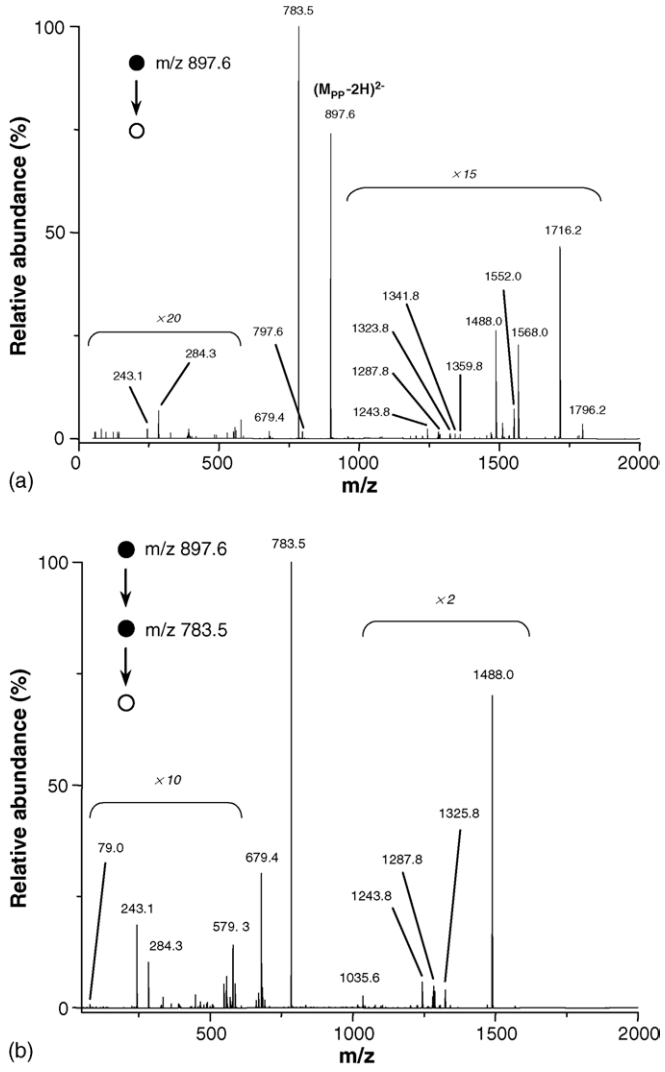

Fig. 8. CID spectra acquired from the doubly charged species $[M_{PP} - 2H]^{2-}$ with (a) ESI-MS/MS mass spectrum of the ion at *m/z* 897.6 (isolation width = 4 u and fragmentation amplitude = 0.5 V_{P-P}) and (b) ESI/MS^3 mass spectrum of the doubly charged daughter ion at *m/z* 783.5 (isolation width = 4 u and fragmentation amplitude = 0.52 V_{P-P}). (Conditions of in-source desolvation: $V_{CE} = -117$ V, $V_{SK1} = -41$ V, LMCO = 62 Th).

at *m/z* 783.5, as shown in the Fig. 8b, displays a minor *m/z* 79.0 ion, characteristic of the HPO_3^- species.

3. Conclusion

ESI-MS^n was known [20,22,23] to be a useful method dedicated to the structural elucidation of endotoxic lipids A by location of fatty acid chains ramified to the common diphosphorylated disaccharide skeleton. By the variation of source and trapping conditions, it is possible to orient the detection of low or high mass to charge ratio ions. It is shown that ester bond cleavage occurred preferentially as compared to the amide bond cleavage. In the same way, the release of phosphate group located at the anomeric position is favored because of the presence of the oxygen atom of the sugar ring. Sequential MS^n CID experiments from de deprotonated species enabled the characterization of O-acylated species. The losses of such O-acylated chains occurred consecutively and/or competitively into the quadrupolar ion trap analyzer, as alkyl carboxylate or alkyl ketene derived species. These processes involve a long distance charge migration. In order to rationalize this behavior by considering only charge-driven processes, as it is expected under low energy dissociation conditions, the formation of intermediate ion–dipole complexes are proposed prior to dissociation. This mechanism is more reasonable than those involving charge-remote processes. Indeed, (i) these processes are not favored under low energy collision energy and (ii) they are expected to lead to characteristic C–C bond and sugar ring cleavages that were not observed. Experimentally the cleavages occurred selectively on the ester and phosphate groups. The presence of two terminal phosphorylated groups on lipid A allowed, in negative ion mode, the generation of doubly deprotonated species. These doubly charged ions were studied, via CID experiments, which provided complementary analytical results by displaying the fatty acids and phosphate ions in the lowest *m/z* range.

Acknowledgment

This work was supported financially by the Centre d'Etudes du Bouchet (CEB/DGA).

References

[1] M.J. Osborn, J.E. Gander, E. Parisi, J. Biol. Chem. 247 (1972) 3973.
[2] J.R. Govan, V. Deretic, Microbiol. Rev. 60 (1996) 539.
[3] O. Lüdertz, M.A. Freudenberg, C. Galanos, V. Lehmann, E.T. Rietschel, D. Shaw, in: S. Razin, S. Rottem (Eds.), Current Topic in Membranes and Transport, vol 17: Membranes Lipids of Prokaryotes, Academic Press, New York, U.S.A., 1982, p. 79.
[4] V. Zähringer, B. Lindner, E.T. Rietschel, in: H. Brade, S.M. Opal, S.N. Vogel, D.C. Morrison (Eds.), Endotoxin in Health and Disease, Marcel Dekker, New York, U.S.A., 1999, p. 93.
[5] O. Holst, in: H. Brade, S.M. Opal, S.N. Vogel, D.C. Morrison (Eds.), Endotoxin in Health and Disease, Marcel Dekker, New York, U.S.A., 1999, p. 115.
[6] P.E. Jansson, in: H. Brade, S.M. Opal, S.N. Vogel, D.C. Morrison (Eds.), Endotoxin in Health and Disease, Marcel Dekker, New York, U.S.A., 1999, p. 155.
[7] U. Zähringer, B. Lindner, E.T. Rietschel, Adv. Carbohydr. Chem. Biochem. 50 (1994) 211.
[8] J. Czaja, W. Jachymek, T. Niedziela, C. Lugowski, E. Aldova, L. Kenne, Eur. J. Biochem. 267 (2000) 1672.
[9] N. Qureshi, K. Takayama, E. Ribi, J. Biol. Chem. 257 (1982) 11808.
[10] N. Qureshi, P. Mascagni, E. Ribi, K. Takayama, J. Biol. Chem. 260 (1985) 5271.
[11] J.-C. Tabet, R.J. Cotter, Anal. Chem. 56 (1984) 1662.
[12] R.J. Cotter, J. Honovich, N. Qureshi, K. Takayama, Biomed. Env. Mass Spectrom. 14 (1987) 591.
[13] U. Seydel, B. Lindner, Springer Ser. Chem. 268 (1993) 12321.
[14] D. Karibian, C. Deprun, L. Szabo, Y. Lebeyec, M. Caroff, Int. J. Mass Spectrom. Ion Processes 111 (1991) 273.
[15] R.B. Cole, L.N. Domelsmith, C.M. David, R.A. Laine, A.J. DeLucca, Rapid Commun. Mass Spectrom. 6 (1992) 616.
[16] I.A. Kaltashov, V. Doroshenko, R.J. Cotter, K. Takayama, N. Qureschi, Anal. Chem. 69 (1997) 2317.
[17] B. Lindner, in: O. Holst (Ed.), Bacterial Toxin Methods and Protocols, Humana Press, Totowa, NJ, 2000, p. 311.

[18] A.K. Harrata, L.N. Domelsmith, R.B. Cole, Biol. Mass Spectrom. 22 (1993) 59.
[19] S.C. Chan, V.N. Reinhold, Anal. Biochem. 218 (1994) 63.
[20] S.M. Boué, R.B. Cole, J. Mass Spectrom. 35 (2000) 361.
[21] Y. Alexeev, T.L. Windus, C.-G. Zhan, D.A. Nixon, Int. J. Quantum Chem. 102 (2005) 775.
[22] A. El-Aneed, J. Banoub, Rapid Commun. Mass Spectrom. 19 (2005) 1683.
[23] F.F. Hsu, J. Turk, J. Am. Soc. Mass Spectrom. 11 (2000) 892.
[24] A. Kussak, A. Weintraub, Anal. Biochem. 307 (2002) 131.
[25] V.A. Kulshin, U. Zahringer, B. Lindner, C.E. Frasch, C.-M. Tsia, B.A. Dimtriev, E.T. Rietschel, J. Bacteriol. 174 (1992) 1793.
[26] Y. Lee, S.-C. Jo, A. Tao, R.G. Cooks, Rapid Commun. Mass Spectrom. 15 (2001) 484.
[27] H. Li, W.R. Plass, G.E. Patterson, R.G. Cooks, J. Mass Spectrom. 37 (2002) 1051.
[28] J.E. McClellan, J.P. Murphy III, J.J. Mulholland, R.A. Yost, Anal. Chem. 74 (2002) 402.
[29] J.P. Murphy III, R.A. Yost, Rapid Commun. Mass Spectrom. 14 (2000) 270.
[30] G. Dobson, J. Murell, D. Despeyroux, F.-L. Wind, J.-C. Tabet, Rapid Commun. Mass Spectrom. 17 (2003) 1657.
[31] M.L. Gross, Int. J. Mass Spectrom. 200 (2000) 611.
[32] M.L. Gross, Int. J. Mass Spectrom. Ion Processes 137 (1992) 118.
[33] C.S. Lee, Y.G. Kim, H.S. Joo, B.G. Kim, J. Mass Spectrom. 39 (2004) 514.
[34] V.H. Wysocki, M.E. Bier, R.G. Cooks, Org. Mass Spectrom. 23 (1988) 627.
[35] F. Fournier, C. Salles, J.C. Tabet, L. Debrauwer, D. Rao, A. Paris, G. Borie, Anal. Chim. Acta 241 (1990) 265.
[36] P. Longevialle, J. C. S. Chem. Commun. (1980) 823.
[37] T. Wyttenbach, B. Paizs, P. Barran, L. Breci, D. Liu, S. Suhai, V.H. Wysocki, M.T. Bowers, J. Am. Chem. Soc. 125 (2003) 13768.